Biochem. J. (2012) **445**, 167–174 (Printed in Great Britain) doi:10.1042/BJ20120504

Architecture of the catalytic HPN motif is conserved in all E2 conjugating enzymes

Benjamin W. COOK and Gary S. SHAW[1]

Department of Biochemistry, The University of Western Ontario, London, ON, Canada, N6A 5C1

E2 conjugating enzymes are the central enzymes in the ubiquitination pathway and are responsible for the transfer of ubiquitin and ubiquitin-like proteins on to target substrates. The secondary structural elements of the catalytic domain of these enzymes is highly conserved, including the sequence conservation of a three-residue HPN (His–Pro–Asn) motif located upstream of the active-site cysteine residue used for ubiquitin conjugation. Despite the vast structural knowledge of E2 enzymes, the catalytic mechanism of these enzymes remains poorly understood, in large part due to variation in the arrangements of the residues in the HPN motif in existing E2 structures. In the present study, we used the E2 enzyme HIP2 to probe the structures of the HPN motif in several other E2 enzymes. A combination of chemical-shift analysis, determination of the histidine protonation states and amide temperature coefficients were used to determine the orientation of the histidine ring and hydrogen-bonding arrangements within the HPN motif. Unlike many three-dimensional structures, we found that a conserved hydrogen bond between the histidine imidazole ring and the asparagine backbone amide proton, a common histidine protonation state, and a common histidine orientation exists for all E2 enzymes examined. These results indicate that the histidine within the HPN motif is orientated to structurally stabilize a tight turn motif in all E2 enzymes and is not orientated to interact with the asparagine side chain as proposed in some mechanisms. These results suggest that a common catalysis mechanism probably exists for all E2 conjugating enzymes to facilitate ubiquitin transfer.

Key words: catalytic pocket, hydrogen bonding, NMR spectroscopy, structure, ubiquitin.

INTRODUCTION

E2 conjugating enzymes are central components in the Ub (ubiquitin) and Ubl (Ub-like) post-translational modification pathways. These enzymes are responsible for accepting a ubiquitin protein from an E1 enzyme and for passing the ubiquitin on to either a substrate (in conjunction with a RING E3 ligase) or directly to a HECT (homologous with E6-associated protein C-terminus) E3 ligase. Thus E2 proteins must possess recognition sequences and structures for both the E1 and E3 enzymes, and potentially a substrate. The tertiary structures of E2 conjugating enzymes are highly conserved, consisting of a central 150 amino acid α/β-fold catalytic domain. Despite the analogous structures of E2 catalytic domains, the sequence identity of E2 enzymes is not well conserved, allowing for a wide diversification of surface interaction sites for various E3 enzymes and substrates. On the other hand, all E2 enzymes contain an essential active-site cysteine residue responsible for the formation of a thiolester linkage with the C-terminal carboxylate of a Ub/Ubl protein. E2 enzymes also contain a highly conserved HPN (His–Pro–Asn) sequence motif found upstream of the active-site cysteine residue. Mutational analysis has found that the asparagine residue within this HPN motif is indispensable for the transfer of the E2 thiolester-linked Ub/Ubl to a lysine residue on either a substrate or growing Ub chain [1,2]. This residue has been proposed to stabilize an oxyanion intermediate formed within an E2∼Ub/Ubl thiolester during the nucleophilic attack of a substrate lysine residue [1–3]. In this mechanism, the asparagine side chain NH_2 group interacts with the thiolester carbonyl to both stabilize the anionic (oxyanion) intermediate and properly orient the carbonyl carbon atom for the nucleophillic attack by a substrate lysine residue. This oxyanion intermediate stabilization would also aid in the transfer of Ub/Ubl from the E2 to the active-site cysteine residue in a HECT E3 ligase forming an E3∼Ub/Ubl thiolester. In some mechanisms, the HPN histidine imidazole ring has been proposed to interact with the HPN asparagine side chain to regulate the electronic nature of the amide group, which would contribute to oxyanion hole stabilization [4]. This electronic affect could be accomplished through either hydrogen bonding or switching between acidic and basic states of histidine. Mutational analysis of the histidine residue within the conserved HPN motif of the E2 enzyme Ubc13 led to a 50% decrease in reactivity, indicating that the histidine contributes to full E2 enzyme activity [1].

High-resolution structures of 25 different human E2 conjugating enzymes have been determined using X-ray crystallography and NMR spectroscopy. Despite this wealth of high-resolution information, there is no consensus structural arrangement of the HPN side chains within the catalytic site. This is surprising since variations within the HPN motif structure would significantly alter the electronic nature within the catalytic pocket and would result in mechanistic inconsistencies within the E2 enzyme family for the transfer of a Ub/Ubl protein on to its substrate. In the present study we analysed the three-dimensional structures of all known E2 enzymes and combined these data with NMR chemical-shift and temperature coefficient measurements to identify the arrangement of the histidine and asparagine residues within the HPN motif.

EXPERIMENTAL

Plasmid construction

Wild-type HIP2 (*UBE2K* in HUGO gene nomenclature) cDNA in a pET28a-LIC vector was a gift from the Structural Genomics Consortium (Toronto, ON, Canada). A C170S substitution

Abbreviations used: BMRB, Biological Magnetic Resonance Bank; DTT, dithiothreitol; HECT, homologous with E6-associated protein C-terminus; HPN, His–Pro–Asn; HSQC, heteronuclear single-quantum coherence; Ni-NTA, Ni^{2+}-nitrilotriacetate; TEV, tobacco etch virus; Ub, ubiquitin; Ubl, Ub-like.

[1] To whom correspondence should be addressed (email gshaw1@uwo.ca).

in HIP2 (HIP2^{C170S}) was introduced using the QuikChange® site-directed mutagenesis protocol (Stratagene). A second round of substitutions was performed using the QuikChange® protocol to convert the protease cleavage site between the N-terminal His_6 tag and HIP2 from thrombin into TEV (tobacco etch virus). Protein substitutions and cleavage site changes were confirmed by DNA sequencing.

Protein expression and purification

Uniformly ^{15}N,^{13}C-labelled Ubc1 (Ubc1Δ^{K93R}), CDC34 (residues 7–182), UbcH8 (UbcH8^{C97,101S}) and UbcH7 (UbcH7^{C17,137S}) proteins were expressed and purified as described previously [5–8]. For the production of uniformly ^{15}N,^{13}C-labelled HIP2^{C170S} (henceforth referred to as HIP2), BL21 CodonPlus(DE3)RIL *Escherichia coli* cells were grown at 37 °C in M9 minimal media containing 1.0 g/l $^{15}NH_4Cl$ and 2.0 g/l [$^{13}C_6$]glucose. Cultures were grown to a D_{600} of 0.6, induced with 0.7 mM IPTG (isopropyl β-D-thiogalactopyranoside) and grown for a further 16–20 h at 16 °C. Cells were harvested and lysed, and soluble lysate containing His_6–HIP2 was subjected to Ni-NTA (Ni^{2+}-nitrilotriacetate) column purification (Qiagen) using 25 mM Tris/HCl, 200 mM NaCl and 1 mM TCEP [tris-(2-carboxyethyl)phosphine] (pH 7.5) with 5, 10 and 200 mM imidazole for binding, washing and elution buffer respectively. The His_6 tag was cleaved using His_6–TEV for 1 h at 22 °C. A second Ni-NTA purification was used to remove His_6–TEV, cleaved His_6 and uncleaved His_6–HIP2 to yield purified HIP2. A final Superdex 75 10/300 GL column (GE Biosciences) was used to remove trace impurities and perform buffer exchange into 25 mM Tris/HCl, 200 mM NaCl, 5 mM DTT (dithiothreitol) and 1 mM EDTA (pH 7.5). Purification of ^{15}N,^{13}C-labelled HIP2 was monitored using SDS/PAGE and the HIP2 molecular mass was confirmed to have 97.3 % isotopic incorporation using electrospray ionization MS [MW_{obs} (observed molecular mass) 23779.0 ± 1.4Da; MW_{calc} (calculated molecular mass) 23812.8 Da].

NMR spectroscopy

All NMR data were acquired using a Varian INOVA 600 MHz spectrometer (Biomolecular NMR Facility, University of Western Ontario, London, ON, Canada) equipped with a triple-resonance cold probe with z gradients. Backbone residue assignments for HIP2 (575 μM) in 25 mM Tris/HCl, 200 mM NaCl, 1 mM EDTA and 5 mM DTT at pH 7.5 in 90 % H_2O/10 % ^2H_2O at 30 °C were made using (^1H-^{15}N)-HSQC (heteronuclear single-quantum coherence) [9], HNCA [10], HN(CO)CA [11], HNCACB [12], CBCA(CO)NH [13], C(CO)NH [14] and HNCO [15] experiments. Chemical-shift values of $C^{\delta 2}$ atoms and $N^{\varepsilon 2}$ atoms in histidine side chains were assigned using (HB)CB(CGCD)HD [16], HCN [17] and ^{13}C-HSQC [18] NMR experiments. To calculate E2 enzyme amide proton temperature coefficients ($\Delta\sigma_{HN}/\Delta T$) [19,20], ($^1H$-$^{15}N$)-HSQC spectra were collected at 5, 10, 15, 20, 25 and 30 °C in 90 % H_2O/10 % ^2H_2O for (i) HIP2 (618 μM) in 25 mM Tris/HCl, 200 mM NaCl, 1 mM EDTA and 5 mM DTT (pH 7.5); (ii) Ubc1 (643 μM) in 25 mM Tris/HCl, 100 mM NaCl, 1 mM EDTA and 1 mM DTT (pH 7.1); (iii) CDC34 (305 μM) in 20 mM Na_2HPO_4, 100 mM NaCl, 1 mM EDTA and 1 mM DTT (pH 7.0); (iv) UbcH7 (649 μM) in 25 mM Tris/HCl, 100 mM NaCl, 1 mM EDTA and 1 mM DTT (pH 7.0); and (v) UbcH8 (634 μM) in 20 mM Na_2HPO_4, 50 mM arginine/glutamate, 100 mM NaCl, 1 mM EDTA and 1 mM DTT (pH 7.0). All data were processed using NMRPipe and NMRDraw [21] and analysed with NMRView [22].

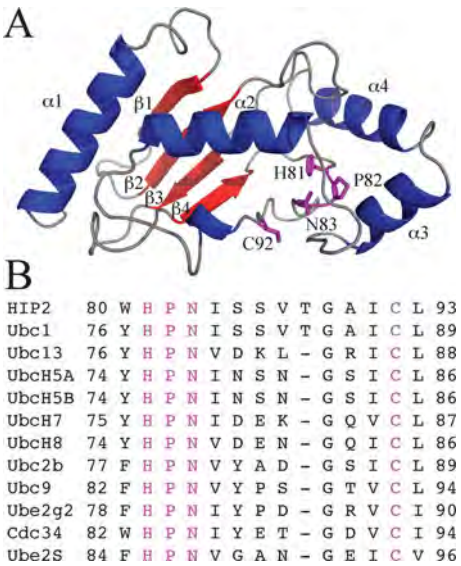

Figure 1 Structure and sequence alignment of the E2 conjugating enzyme

(**A**) Representative three-dimensional structure of the catalytic core for the E2 protein showing a ribbon diagram for HIP2 (PDB code 2BEP). The structure shows α-helices (blue) and β-strands (red) whose structure is conserved in all E2 enzymes. Side chains are shown for the HPN motif [H81 (His^{81}), P82 (Pro^{82}) and N83 (Asn^{83})] and active site C92 (Cys^{92}) residues. (**B**) Sequence alignment of twelve E2 conjugating enzymes showing the conservation of the HPN motif and catalytic cysteine residue. Ubc1 is the *Saccharomyces cerevisiae* homologue of HIP2, with all other proteins representing different *Homo sapiens* E2 enzymes.

RESULTS

Structures of 25 out of the 34 human E2 enzymes have been determined using X-ray crystallography or NMR spectroscopy (81 structures in total). These structures reveal that the catalytic domain of all E2 enzymes is composed of an α/β fold, comprising four well-defined α-helices (α1–α4) and four β-strands (β1–β4) (Figure 1A). This conserved domain contains an active-site catalytic cysteine residue that forms a thiolester linkage with the C-terminus of Ub/Ubl proteins. The catalytic cysteine residue is found within a region of the protein that possesses little regular secondary structure with the exception of a short poorly defined helix neighbouring the cysteine residue. Also located within this region is the HPN motif, which is found in 65 % of all E2 enzymes and is 100 % conserved within the twelve E2 enzymes that have both high-resolution structure solutions and NMR chemical-shift assignment data (Figure 1B). This HPN motif forms a tight turn adjacent to the active-site cysteine residue. The asparagine residue in this HPN motif has been suggested to stabilize an oxyanion intermediate formed on the E2-Ub/Ubl thiolester during nucleophilic attack by a substrate lysine [1–3].

Despite the sequence conservation of the HPN motif in E2 proteins and its integral role in catalysis, it is surprising that important structural differences exist within this motif in the high-resolution structures available. These differences were initially observed during the comparison of multiple high-resolution structures of the E2 enzyme HIP2. Two structures of HIP2 (PDB codes 2BEP and 2BF8) indicate the backbone amide proton (H^N) of Asn^{83} is involved in a hydrogen bond to the deprotonated $N^{\delta 1}$ nitrogen atom (ε-tautomer) of the His^{81} side chain (Figure 2A). In contrast, other structures of HIP2 (PDB codes 3E46, 1YLA, 3K9P, 3K9O and 2O25) show a near mirror image of the His^{81} imidazole ring, resulting in an alternative hydrogen bond between the protonated $N^{\varepsilon 2}$ nitrogen and the side-chain amide oxygen ($O^{\delta 1}$) from Asn^{83} (Figure 2B). In this second arrangement, the Asn^{83}

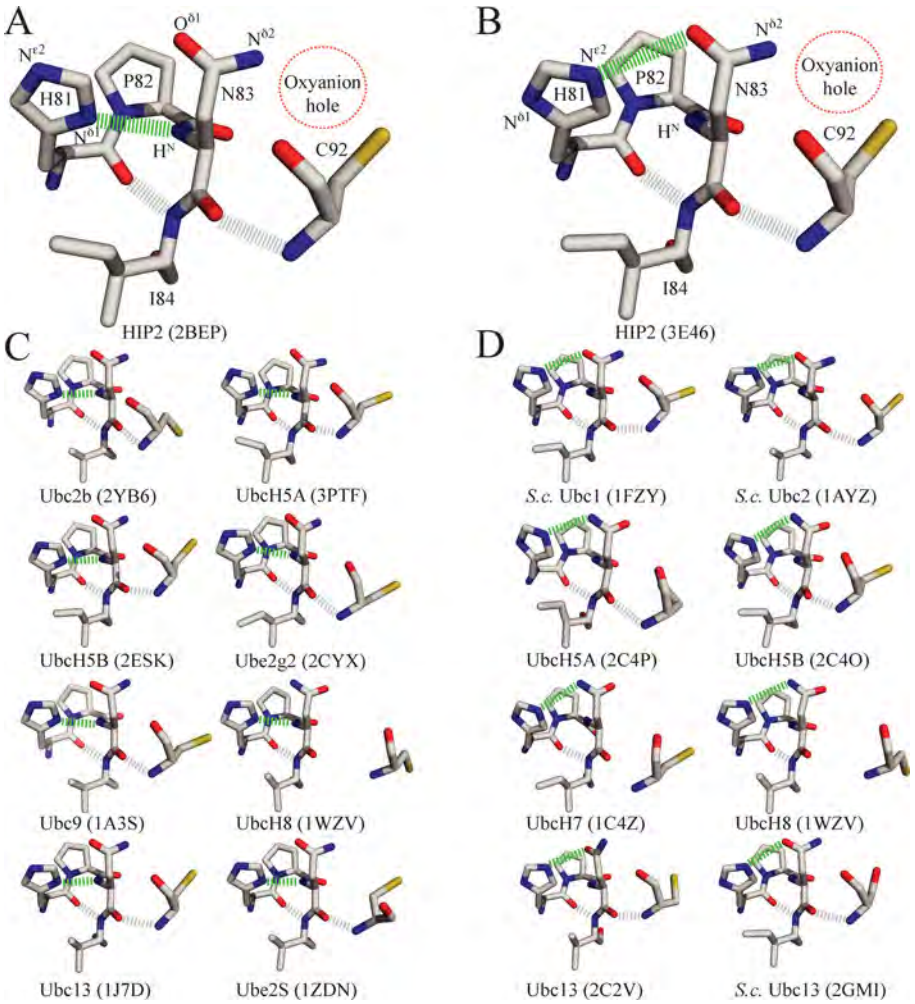

Figure 2 Structures of alternative histidine side-chain configurations for the HPN motif in several E2 conjugating enzymes

Two major configurations of the HPN motif of the E2 conjugating enzyme HIP2 are shown depicting (**A**) a hydrogen bond between $N^{\delta 1}$ of the H81 (His^{81}) side chain with the backbone amide proton (H^N) from N83 (Asn^{83}) and (**B**) a hydrogen bond between $N^{\varepsilon 2}$ of the H81 (His^{81}) side chain and the side chain $O^{\delta 1}$ from N83 (Asn^{83}). (**C**) Ubc2b, UbcH5A, UbcH5B, Ube2g2, Ubc9, UbcH8 (model A), Ubc13 and Ube2S adopt HPN motif hydrogen-bonding patterns similar to (**A**). Structures adopting configurations equivalent to (**C**), but not shown, include HIP2 (PDB code 2BF8), Ubc2b (PDB code 2YBF), UbcH5A (PDB codes 3OJ4 and 2YHO), UbcH5B (PDB code 1UR6, 3A33, 3TGD, 2CLW, 3L1Y, 3JVZ and 3EB6), Ube2g2 (PDB codes 3FSH and 3H8K), Ubc9 (PDB codes 2GRN, 1Z5S, 1U9B, 2O25, 2PE6, 1KPS, 1U9A and 2VRR), UbcH8 (PDB codes 1WZW and 2KJH), Ubc13 (PDB codes 3HCT and 3HCU), CDC34 (PDB codes 2OB4 and 3RZ3), Ube2U (PDB code 1YRV), UbcH10 (PDB code 1I7K), UbcH5c (PDB codes 3RPG and 3L1Z), Ube2g1 (PDB code 2AWF) and Ube2H (PDB code 2Z5D). (**D**) *S.c.* (*S. cerevisiae*) Ubc1, *S.c.* Ubc2, UbcH5A, UbcH5B, UbcH7, UbcH8 (model B), Ubc13 (model E) and *S.c.* Ubc13 adopt HPN motif structures that retain interactions between the histidine and asparagine side chains similar to (**B**). Structures adopting configurations equivalent to (**D**), but not shown, include HIP2 (PDB codes 1YLA, 3K9P, 2O25 and 3K9O), Ubc1 (PDB codes 1TTE and 1FXT), Ubc2b (PDB code 2Y4W), UbcH5B (PDB code 1W4U), UbcH7 (PDB code 1FBV) and Ubc13 (PDB codes 1JBB and 1JAT). Proposed hydrogen bonds are shown with grey or green bars. Oxygen, nitrogen, carbon and sulfur atoms are coloured red, blue, grey and yellow respectively. The PDB code for each respective structure is listed beside the E2 enzyme name.

backbone amide proton no longer forms a hydrogen bond with any of its neighbouring residues. Although illustrated for HIP2, these architectural differences are representative of all E2 enzyme structures. A survey of three-dimensional E2 enzyme structures from the PDB indicates that 54 structures adopt the HPN histidine ring orientation, consistent with Figure 2(A), 23 structures adopt the HPN histidine ring orientation, consistent with Figure 2(B), and four structures show variable orientations. Representative structures of each orientation are shown in Figures 2(C) and 2(D). Interestingly, both orientations of the histidine ring have been observed in independent structures of HIP2, UbcH5A, UbcH5B, UbcH8 and Ubc13 (Figure 2). Analysis of the experimental conditions for each three-dimensional structure revealed there was no obvious trend in salt concentration, pH or temperature that resulted in a structure adopting one or the other orientation shown in Figures 2(A) or 2(B) (see Supplementary Table S1 at http://www.BiochemJ.org/bj/445/bj4450167add.htm). For example, HIP2 structures are found with the histidine ring orientation shown in Figure 2(B) at pH 6 (PDB code 3E46) and pH 8.5 (PDB code 3K9C), whereas UbcH5B structures in both orientations occur near pH 4.5. These results show that the difference in structures with regard to the HPN motif is not a result of experimental crystallization or NMR conditions used during the structure determination.

Although both histidine orientations shown in Figure 2 are possible, an interaction between the histidine and asparagine side chains within the HPN motif (Figure 2B) has been suggested to have a catalytic role in stabilizing the oxyanion hole [4]. Disruption of the proposed oxyanion hole can be caused when the orientation of the asparagine side chain becomes flipped, in some cases due to hydrogen bonding using the δ-tautomer of the HPN histidine (Figure 2D). Given the functional importance

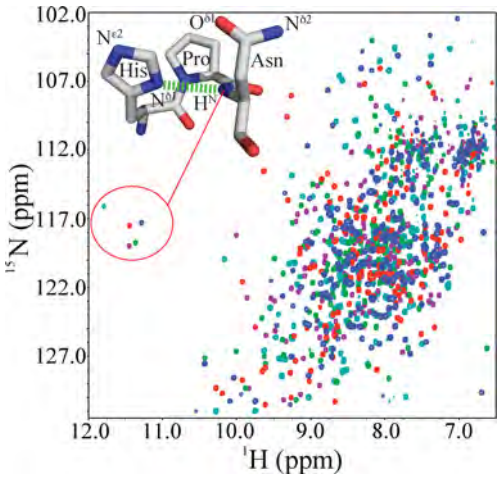

Figure 3 Similarity of the chemical shifts for the HPN asparagine amide resonances of several E2 enzymes

The superimposed (^{1}H-^{15}N)-HSQC spectra of HIP2 [N83 (Asn^{83}), blue], Ubc1 [N79 (Asn^{79}), red], UbcH7 [N78 (Asn^{78}), green], UbcH8 [N77 (Asn^{77}), purple] and CDC34 [N85 (Asn^{85}), teal] are shown with the downfield-shifted HPN asparagine amide resonances indicated (red circle). All spectra were collected at 30 °C using protein concentrations between 300 and 650 μM. The inset shows the proposed hydrogen bond between the HPN asparagine amide nitrogen and the histidine $N^{\delta 1}$ atoms.

of the HPN motif and the significant discrepancies between structures, identifying the arrangement of the histidine ring, its proper tautomeric state, and its hydrogen-bonding network with the asparagine or other residues will be important in proposing mechanisms for catalysis across the family of E2 enzymes.

Conserved environment of the HPN asparagine residue in E2 enzymes

As a first step towards identifying potential hydrogen-bonding patterns in the HPN motif, the backbone NH resonance assignments for HIP2 were completed using standard triple-resonance experiments. The high quality (^{1}H-^{15}N)-HSQC spectrum of HIP2 showed that 175 out of 187 (94 %) ^{1}H and ^{15}N amide resonances (non-proline) have been assigned (see Supplementary Figure S1 at http://www.BiochemJ.org/bj/445/bj4450167add.htm). Unassigned residues (Met^{1}, Asn^{3}, Glu^{20}, Thr^{22}, Asp^{33}, Glu^{34}, Phe^{36}, Glu^{66}, Ala^{128}, Val^{157}, Ser^{159} and Glu^{161}) are located in highly flexible and solvent-exposed regions and were probably unobservable due to fast amide exchange with the solvent. NMR chemical-shift index analysis (results not shown) [23,24] indicated that the secondary structure of HIP2 contains four α-helices and four β-sheets, consistent with the X-ray crystal structures.

A unique feature of the (^{1}H-^{15}N)-HSQC spectrum of HIP2 is the distinctly downfield-shifted amide proton resonance for Asn^{83} (H^{N}, 11.30 p.p.m.; ^{15}N, 117.4 p.p.m.; Figure 3), located within the HPN motif. The amide proton resonance for Asn^{83} is shifted 4.7 S.D. values from the expected BMRB (Biological Magnetic Resonance Bank) average of 8.34 ± 0.63 p.p.m., indicating that it is in a unique environment. An analogous observation was first made for the HIP2 homologue Ubc1, which has a similar resonance position for the corresponding residue Asn^{79} [25,26]. Furthermore, (^{1}H-^{15}N)-HSQC spectra of previously described E2 enzymes Ubc1 [25,26], UBE2L3 (UbcH7) [8], UBE2L6 (UbcH8) [7] and CDC34 (D.E. Spratt and G.S. Shaw, unpublished work) also demonstrate the conservation of this distinctly downfield-shifted asparagine amide proton (Figure 3). A survey of the BMRB revealed that NMR chemical-shift assignments are available for seven other E2 enzymes including UBE2B (Ubc2b) [27], UBE2D1 (UbcH5A) [28], UBE2D2 (UbcH5B) [29], UBE2G2 (Ubc7) [30], UBE2I (Ubc9) [31], UBE2N (Ubc13) [32] and UBE2S (Ube2S) [33]. Without exception, these E2 conjugating enzymes all possess the same distinctive downfield-shifted amide proton resonance for the asparagine residue within the HPN motif (Table 1). Therefore, unlike the three-dimensional structures, these results indicate that a similar environment exists for the backbone amide proton of the asparagine residue within the HPN motif of all E2 conjugating enzymes.

The downfield-shifted asparagine amide proton resonance within the HPN motif can be rationalized by a close inspection of a subset of available E2 conjugating enzyme structures. Hydrogen bonds are known to have a significant deshielding effect on amide protons [34]. In HIP2, the highly deshielded Asn^{83} amide backbone proton is consistent with the His^{81} $N^{\delta 1}$ hydrogen bond shown in Figure 2(A), whereas this hydrogen bond is absent in Figure 2(B). The geometry of this hydrogen bond also places the Asn^{83} amide (H^{N}) proton in plane with the His^{81} aromatic ring current, which also contributes to the deshielding effect [35]. Since the E2 conjugating enzymes Ubc1, Ubc2b, UbcH5A, UbcH5B, Ube2g2, Ubc9, UbcH7, UbcH8, Ubc13, CDC34 and Ube2S all contain a similarly distinct asparagine backbone amide proton chemical shift (Table 1), it is likely that all of these enzymes adopt a structure similar to that shown in Figure 2(A). A similar hydrogen bond between a backbone amide proton and a histidine $N^{\delta 1}$ atom has previously been observed in the unrelated protein BsCM (*Bacillus subtilis* chorismate mutase) [36], where the amide proton chemical shift for Arg^{7} was reported at 11.88 p.p.m.

Histidine protonation state within the HPN motif

One requirement for a hydrogen bond between the H^{N} atom and $N^{\delta 1}$ atoms of the asparagine and histidine residues within the HPN motif is that the histidine residue must exist as an ε-tautomer ($N^{\delta 1}$ deprotonated, $N^{\varepsilon 2}$ protonated). In order to identify the tautomeric state of the histidine ring in the HPN motif, we conducted NMR experiments aimed at identifying the protonation states of histidine $N^{\delta 1}$ and $N^{\varepsilon 2}$ atoms for several E2 enzymes including HIP2, Ubc1, UbcH7, UbcH8 and CDC34. The tautomeric state of a histidine side chain can be identified by several key chemical-shift values for the atoms within the imidazole ring, since these atoms are sensitive to the protonation state. The chemical shifts of the $N^{\delta 1}$ or $N^{\varepsilon 2}$ atoms have average values near 165 p.p.m. in the deprotonated state, shift significantly downfield by approximately 85 p.p.m. (~250 p.p.m.) in the protonated state, and shift moderately by approximately 10 p.p.m. (~175 p.p.m.) if the imidazole ring becomes positively charged (both $N^{\delta 1}$ and $N^{\varepsilon 2}$ protonated) [17,37–40]. The chemical shift of $C^{\delta 2}$ is also diagnostic of the histidine tautomeric form, as the chemical shift of this atom is <122 p.p.m. for the ε-tautomer ($N^{\delta 1}$ unprotonated) and >122 p.p.m. for the δ-tautomer ($N^{\varepsilon 2}$ unprotonated) [17,41]. The assignment of chemical-shift values of $C^{\delta 2}$ atoms and most $N^{\varepsilon 2}$ atoms of the histidine residues within the HPN motif for several E2 enzymes were acquired using (HB)CB(CGCD)HD [16], HCN [17] and (^{1}H-^{13}C)-HSQC [18] NMR experiments. These HPN histidine side-chain assignments were combined with those previously determined for UbcH7, Ube2g2 and Ube2B (Table 1). The data show that there is remarkable agreement between the histidine chemical-shift values reported for the $C^{\delta 2}$ and $N^{\varepsilon 2}$ atoms within the HPN motif. All chemical shifts observed for $C^{\delta 2}$ are between 115.9 and 118.2 p.p.m., consistent with the values expected for the ε-tautomeric state. All $N^{\varepsilon 2}$ assignments

Table 1 Resonance assignments for HPN motif residues in E2 conjugating enzymes

Chemical shifts are reported in p.p.m. in relation to a DSS (2,2-dimethyl-2-silapentane-5-sulfonate sodium salt) reference.

		Asparagine		Histidine			
Protein	PDB code(s)	$^{1}H^{N}$	^{15}N	$N^{\delta1}$	$C^{\delta2}$	$N^{\varepsilon2}$	BMRB
HIP2 (*UBE2K*)	1YLA, 2BEP, 3E46, 3K9P	11.30*	117.4	–	117.9†	–	–
		11.27*	117.4	–	–	–	17362
Ubc1 (yeast)	1FZY, 1TTE	11.45*	117.6	–	118.2†	164.3†	6202
Ubc2b (UBE2B)	2Y4W, 2YB6	11.28*	114.6	–	117.5‡	–	5038
UbcH5A (UBE2D1)	2C4P, 3PTF	11.39*	117.5	–	–	–	6584
UbcH5B (UBE2D2)	2ESK, 2C4O	11.53*	118.4	–	–	–	6277
Ube2g2 (UBE2G2)	2CYX, 2KLY	11.04*	114.8	255.0§	115.9§	165.0§	16404
Ubc9 (UBE2I)	1A3S	11.62*	115.7	–	–	–	4132
UbcH7 (UBE2L3)	1C4Z	11.38*	118.8	–	118.0†	167.0†	15498
UbcH8 (UBE2L6)	1WZV, 2KJH	11.48*	118.9	–	117.7†	166.9†	16321
Ubc13 (UBE2N)	1J7D, 2C2V	10.90*	118.0	–	–	–	15092
CDC34 (UBE2R1)	2OB4	11.84*	116.2	–	117.7†	–	–
Ube2S (UBE2S)	1ZDN	11.44*	116.8	–	–	–	17437

*Unique chemical shifts; 4–5.5 S.D. values from the expected value of 8.34 p.p.m. (BMRB).
†Results from the present study from HIP2, UbcH8, UbcH7, Ubc1 and CDC34.
‡Data from [29].
§Data from [30].

were found between 164.3 and 167.0 p.p.m. within 2 p.p.m. of ~165 p.p.m. indicating that the $N^{\varepsilon2}$ atom is protonated. Correspondingly the $N^{\delta1}$ atom must be deprotonated, although this resonance could only be observed directly for Ube2g2 [30]. Therefore the chemical shift values observed in Table 1 are consistent with an ε-tautomeric state in all E2 enzymes examined. This analysis is in agreement with conclusions for Ube2g2 where the HPN histidine residue was found to be exclusively in the ε-tautomer over a broad pH range of 6.5–9.5 [30].

These results indicate that the HPN histidine residue adopts the ε-tautomeric form needed to provide a deprotonated $N^{\delta1}$ atom for hydrogen bonding. Furthermore, the conserved deshielded H^{N} amide backbone proton for the asparagine residue is conserved in all E2 enzymes (Table 1). These data support a structure where all E2 enzymes possess a hydrogen bond similar to that depicted between His^{81} $N^{\delta1}$ and Asn^{83} H^{N} in HIP2 shown in Figure 2(A).

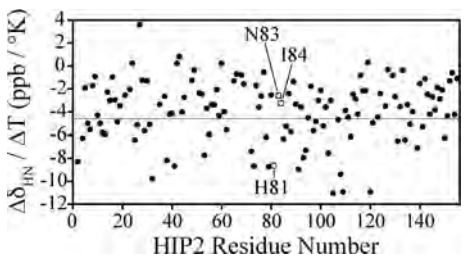

Figure 4 Amide proton temperature coefficients for the catalytic core domain of HIP2

(^{1}H-^{15}N)-HSQC spectra of HIP2 were collected at 5, 10, 15, 20, 25 and 30 °C and amide proton chemical shifts were plotted as a function of temperature to obtain $\Delta\sigma_{HN}/\Delta T$. Some residues are absent from the plot due to excessive broadening at lower temperatures. A dotted line is shown at −4.6 p.p.b./K. Values above this line are consistent with the presence of amide proton hydrogen bonding.

NMR temperature coefficients support a conserved hydrogen bond within the HPN motif

Backbone amide protons that participate in hydrogen bonds can be identified within a protein by measuring the change in chemical shift as the temperature is adjusted. Amide temperature coefficients ($\Delta\sigma_{HN}/\Delta T$) were measured for UbcH7, UbcH8, HIP2, Ubc1 and CDC34 by collecting a series of HSQC spectra between 5 and 30 °C. As shown for HIP2 (Figures 4 and 5), linear chemical-shift profiles are found for His^{81} and Asn^{83} within the HPN motif. The amide temperature coefficients measured for HIP2 (Figure 4) show a large number of residues with coefficients larger than −4.6 p.p.b./K, a value proposed to be indicative of hydrogen bonding [19,20]. This observation is consistent with the secondary structure of HIP2, which shows four α-helices and four β-strands within its first 150 residues that display a network of hydrogen bonds. Within the HPN motif of HIP2, Asn^{83} ($\Delta\sigma_{HN}/\Delta T = -2.58$ p.p.b./K) falls well within the range expected for a hydrogen bond [19,20]. As expected from an examination of HIP2 structures, the temperature coefficient for His^{81} ($\Delta\sigma_{HN}/\Delta T = -8.64$) suggests that its amide is not involved in a hydrogen bond regardless of the histidine imidazole ring orientation (Figure 2). The arrangements of the HPN motif in all E2 structures (Figure 2) also show a hydrogen bond between the backbone amide proton from the residue immediately following the HPN motif (Ile^{84} in HIP2), to the backbone carboxylate oxygen of the histidine residue (His^{81} in HIP2). The temperature coefficient for the Ile^{84} amide proton measured 3.24 p.p.b./K (Figure 4), indicative of a hydrogen bond.

Similar results were observed for other E2 enzymes examined. In all cases, the HPN histidine backbone amide protons (H^{N}) for UbcH7, UbcH8, Ubc1 and CDC34 (Lys^{80} used as His^{83} was unobservable) displayed large chemical-shift changes ($\Delta\sigma_{HN}/\Delta T = -14.70$, −12.19, −8.26 and −6.75 p.p.b./K respectively) inconsistent with hydrogen bonding (Figure 5). In contrast the HPN asparagine amide protons for UbcH7, UbcH8, Ubc1 and CDC34 displayed much smaller chemical-shift changes ($\Delta\sigma_{HN}/\Delta T = -2.81$, −2.40, −4.55 and −2.72 p.p.b./K respectively) indicative of hydrogen bonding. Hydrogen bonding was also confirmed for the residue following the HPN motif (analogous to Ile^{84} in HIP2) in UbcH7, UbcH8, Ubc1 and CDC34 based on small temperature coefficients ($\Delta\sigma_{HN}/\Delta T = -1.30$, −0.80, −1.63 and −1.62 p.p.b./K respectively). Taken together, these results from the same structural region of five different E2

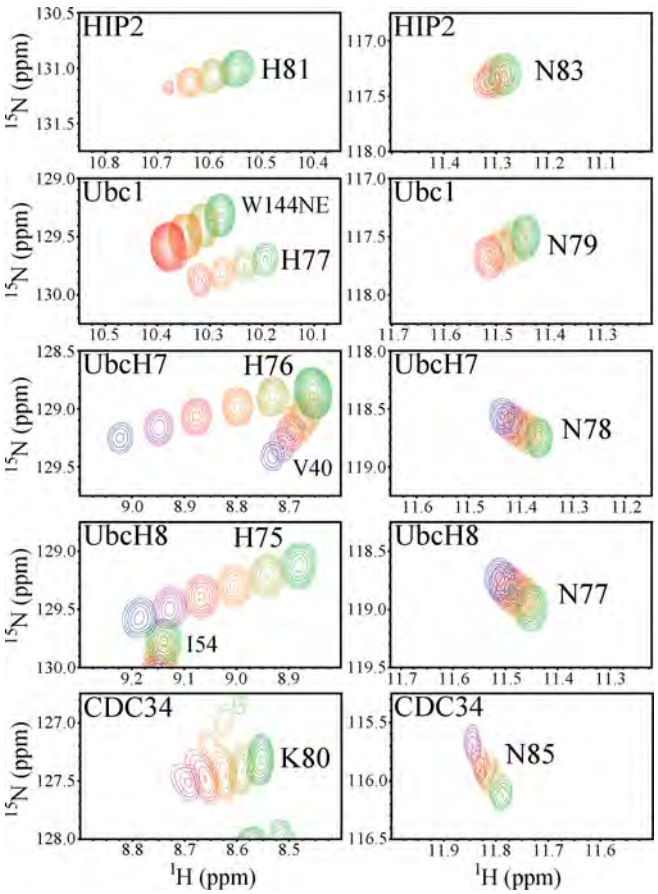

Figure 5 NMR temperature titrations of E2 enzymes used to acquire amide proton temperature coefficients

(^{1}H-^{15}N)-HSQC spectra of HIP2, UbcH7, UbcH8, Ubc1 and Cdc34 were collected at 5 °C (blue), 10 °C (purple), 15 °C (red), 20 °C (orange), 25 °C (yellow) and 30 °C (green). The change in H^N chemical shift was measured against temperature change ($\Delta\sigma_{HN}/\Delta T$). All spectra were collected at 600 MHz using ^{15}N,^{13}C-labelled proteins.

enzymes indicate that all of these E2 enzymes adopt the hydrogen-bonding configuration depicted in Figure 2(A) (shown for His^{81} $N^{\delta1}$ and Asn^{83} H^N in HIP2).

Re-investigation of structural data suggests a revised histidine orientation

Since our NMR results indicated consistent hydrogen-bonding arrangements between the histidine side chain $N^{\delta1}$ atom and the asparagine backbone amide proton, we re-investigated this portion of the structure for all 81 E2 structures in the PDB. Each structure was analysed manually to measure the existing hydrogen bond and using MolProbity [42] to assess the orientation of the histidine ring in a given set of co-ordinates (see Supplementary Table S2 at http://www.BiochemJ.org/bj/445/bj4450167add.htm). This analysis showed that hydrogen bonds, consistent with Figure 2(A), were on average shorter [histidine $N^{\delta1}$ to asparagine N: 2.94 Å (1 Å = 0.1 nm)] than alternative structures shown in Figure 2(B) (histidine $N^{\varepsilon2}$ to Asn $N^{\delta2}$ or $O^{\delta1}$: 3.25Å). Furthermore, structural examination using Molprobity recommended flipping the histidine side chain in 21 out of 23 structures from the histidine orientation shown in Figure 2(B) to that for the arrangement depicted in Figure 2(A). These two analysis steps further support a hydrogen-bonding configuration for all E2 enzymes that involves the histidine side chain $N^{\delta1}$ atom and the asparagine backbone amide proton (H^N) within the HPN motif.

DISCUSSION

The variations in the orientation of the histidine ring within the HPN motif, shown in multiple three-dimensional structures of E2 enzymes to date, is surprising given the importance of these residues to Ub transfer. Although some mechanistic details have been proposed for Ubc9 [2,3,43], a common framework suggested by the consensus sequences of E2 enzymes near the catalytic site has not been possible due in part to the structural differences within these proteins.

However, NMR studies performed on 12 different E2 conjugating enzymes consistently yield a uniquely downfield-shifted backbone amide proton resonance for the HPN asparagine residue. These results support a single histidine ring orientation, whereby a hydrogen bond is formed between the HPN histidine $N^{\delta1}$ atom and asparagine amide proton (H^N). In addition, seven E2 enzymes display chemical shifts that support an ε-tautomeric histidine, and five E2 enzymes have amide temperature coefficients consistent with the presence of a hydrogen bond to the asparagine amide proton. This HPN architecture is supported by previous computer modelling experiments that optimize the HPN hydrogen-bonding network [44]. The E2 enzymes assessed cover a broad range of isotypes and functions, and include class I E2 enzymes (Ubc2b, UbcH5A, UbcH5B, Ube2g2, Ubc9, UbcH7, UbcH8, Ubc13 and Ube2S), class II enzymes (HIP2, Ubc1, CDC34), E2 enzymes containing an additional acidic loop (CDC34 and Ube2g2), and Ubc9 involved in SUMOylation. Unlike the three-dimensional structures currently available, these results provide strong evidence that all E2 enzymes contain a hydrogen bond between the histidine side chain $N^{\delta1}$ atom and the asparagine backbone amide proton (H^N) within the HPN motif. This observation would point to a common mechanism for Ub transfer used by all E2 enzymes.

Relationship to existing mechanisms

Many of the high-resolution E2 structures depict the protonated $N^{\varepsilon2}$ atom of the HPN histidine residue with a hydrogen bond to the $O^{\delta1}$ of the asparagine amide side chain. This interaction would affect the electronic nature of the amide amino-group and could contribute to stabilizing the anionic (oxyanion) intermediate of the thiolester and properly orientating the thiolester for nucleophillic attack by a substrate lysine [4]. In this work the identification of a hydrogen bond between the HPN histidine $N^{\delta1}$ atom and HPN asparagine amide proton (H^N) precludes the interaction between the histidine side chain and the asparagine side chain in E2 enzymes. This observation suggests that histidine is not directly involved in stabilizing a thiolester intermediate.

The specific HPN hydrogen bond identified in the present study is also retained during thiolester formation, as the distinct downfield shift of the asparagine amide proton is maintained in Ubc1 upon Ubc1∼Ub thiolester formation (K.S. Hamilton and G.S. Shaw, unpublished work). A similar conclusion is reached for Ubc13∼Ub ester bond formation [45] and disulfide mimics between Ub and several E2 enzymes (HIP2–Ub, CDC34–Ub, UbcH8–Ub) (B.W. Cook and G.S. Shaw, unpublished work; D.E. Spratt and G.S. Shaw, unpublished work) [7]. These results show that significant orientational changes, rotation or a change in the protonation state of the histidine side chain does not occur upon E2∼Ub thiolester intermediate formation. These results support

the notion that the histidine residue is not directly used for E2∼Ub thiolester intermediate stabilization.

A detailed active-site mechanism has been proposed for the E2 enyzme Ubc9 [2,3,43]. This mechanism, using the same specific HPN hydrogen bond determined in the present study, has shown Ubc9 in complex with a SUMOylated (Ubl-linked) substrate where the HPN asparagine residue is positioned within hydrogen-bonding distance (3 Å) of the carbonyl of the peptide bond (formerly thiolester) after nucleophillic attack to a substrate lysine residue [43]. Additionally, the structure of a UbcH5b∼Ub ester, which also incorporates the same HPN hydrogen bond, positions the HPN asparagine residue within hydrogen-bonding distance to stabilize the thiolester oxyanion and orientate it for nucleophilic attack [46]. These two structures indicate that the HPN asparagine side chain can act catalytically to stabilize a thiolester intermediate while incorporating the specific HPN hydrogen bond determined in the present study. Since the present study implicates a common hydrogen bond for all E2 enzymes, this would suggest that the mechanism proposed for Ubc9 may be a more general mode of catalysis used by other E2 enzymes as well.

Role of the histidine residue in the HPN motif

We propose that the central role of the HPN histidine residue is to hydrogen bond to the asparagine backbone to stabilize the HPN tight turn architecture. In this role, histidine would act as a structural participant only and have little direct influence on catalysis of Ub transfer. When the HPN histidine $N^{\delta 1}$ atom hydrogen bonds to the asparagine amide proton (H^N), an additional hydrogen bond is formed between the histidine protonated $N^{\varepsilon 2}$ nitrogen and a backbone carbonyl on the C-terminal end of $\alpha 2$. Additionally, this histidine residue is predominantly buried in the hydrophobic centre of E2 enzymes. These factors all contribute to a conserved positioning of the HPN motif near the active site. Previous experiments where the HPN histidine residue was substituted with alanine in the E2 enzyme Ubc13 resulted in >90 % insoluble protein expression [1]. These results may indicate that arrangement of the conserved HPN histidine is crucial for structural stability, as the removal of histidine would disrupt the histidine interaction with $\alpha 2$ and disrupt the HPN tight turn architecture afforded by the asparagine hydrogen bond. The result implies that the histidine residue is not used catalytically, but that active-site instability might reduce enzyme activity [1]. We propose that a highly stable HPN structure is dependent on the specific histidine orientation determined in the present study, and that this architecture properly positions the HPN asparagine for interactions with Ub/Ubl thiolester intermediates to allow conjugation of Ub/Ubl proteins on to substrates.

AUTHOR CONTRIBUTION

Benjamin Cook designed and performed experiments, analysed results and wrote the paper; Gary Shaw designed the study, analysed results and wrote the paper.

ACKNOWLEDGEMENTS

We thank Anne Rintala-Dempsey for maintenance of the Biomolecular NMR Facility.

FUNDING

This work was supported by the Canadian Institutes of Health Research [grant number MOP-14606], the Canadian Cancer Society [grant number 018414] and the Canada Research Chairs Program (to G.S.S.).

REFERENCES

1 Wu, P. Y., Hanlon, M., Eddins, M., Tsui, C., Rogers, R. S., Jensen, J. P., Matunis, M. J., Weissman, A. M., Wolberger, C. and Pickart, C. M. (2003) A conserved catalytic residue in the ubiquitin-conjugating enzyme family. EMBO J. **22**, 5241–5250
2 Yunus, A. A. and Lima, C. D. (2006) Lysine activation and functional analysis of E2-mediated conjugation in the SUMO pathway. Nat. Struct. Mol. Biol. **13**, 491–499
3 Reverter, D. and Lima, C. D. (2005) Insights into E3 ligase activity revealed by a SUMO-RanGAP1-Ubc9-Nup358 complex. Nature **435**, 687–692
4 Burroughs, A. M., Jaffee, M., Iyer, L. M. and Aravind, L. (2008) Anatomy of the E2 ligase fold: implications for enzymology and evolution of ubiquitin/Ub-like protein conjugation. J. Struct. Biol. **162**, 205–218
5 Hodgins, R., Gwozd, C., Arnason, T., Cummings, M. and Ellison, M. J. (1996) The tail of a ubiquitin-conjugating enzyme redirects multi-ubiquitin chain synthesis from the lysine 48-linked configuration to a novel non-lysine-linked form. J. Biol. Chem. **271**, 28766–28771
6 Spratt, D. E. and Shaw, G. S. (2011) Association of the disordered C-terminus of CDC34 with a catalytically bound ubiquitin. J. Mol. Biol. **407**, 425–438
7 Serniwka, S. A. and Shaw, G. S. (2009) The structure of the UbcH8-ubiquitin complex shows a unique ubiquitin interaction site. Biochemistry **48**, 12169–12179
8 Serniwka, S. A. and Shaw, G. S. (2008) ^{1}H, ^{13}C and ^{15}N resonance assignments for the human E2 conjugating enzyme, UbcH7. Biomol. NMR Assign. **2**, 21–23
9 Kay, L. E., Keifer, P. and Saarinen, T. (1992) Pure absorption gradient enhanced heteronuclear single quantum correlation spectroscopy with improved sensitivity. J. Am. Chem. Soc. **114**, 10663–10665
10 Grzesiek, S. and Bax, A. (1992) An efficient method for sequential backbone assignment of medium-sized isotopically enriched proteins. J. Magn. Reson. **99**, 201–207
11 Bax, A. and Ikura, M. (1991) An efficient 3D NMR technique for correlating the proton and ^{15}N backbone amide resonances with the α-carbon of the preceding residue in uniformly $^{15}N/^{13}C$ enriched proteins. J. Biomol. NMR **1**, 99–104
12 Wittekind, M. and Mueller, L. (1993) HNCACB, a high-sensitivity 3D NMR experiment to correlate amide-proton and nitrogen resonances with the α-carbon and β-carbon resonances in proteins. J. Magn. Reson. **B101**, 201–205
13 Grzesiek, S. and Bax, A. (1992) Correlating backbone amide and side-chain resonances in larger proteins by multiple relayed triple resonance NMR. J. Am. Chem. Soc. **114**, 6291–6293
14 Grzesiek, S., Anglister, J. and Bax, A. (1993) Correlation of backbone amide and aliphatic side-chain resonances in C-13/N-15-enriched proteins by isotropic mixing of C-13 magnetization. J. Magn. Reson. **B101**, 114–119
15 Kay, L. E., Xu, G. Y. and Yamazaki, T. (1994) Enhanced-sensitivity triple-resonance spectroscopy with minimal H2O saturation. J. Magn. Reson. **A109**, 129–133
16 Yamazaki, T., Forman-Kay, J. D. and Kay, L. E. (1993) 2-Dimensional NMR experiments for correlating C-13-β and H-1-δ/ε chemical-shifts of aromatic residues in C-13-labeled proteins via scalar couplings. J. Am. Chem. Soc. **115**, 11054–11055
17 Sudmeier, J. L., Ash, E. L., Gunther, U. L., Luo, X., Bullock, P. A. and Bachovchin, W. W. (1996) HCN, a triple-resonance NMR technique for selective observation of histidine and tryptophan side chains in $^{13}C/^{15}N$-labeled proteins. J. Magn. Reson. **B113**, 236–247
18 John, B. K., Plant, D. and Hurd, R. E. (1993) Improved proton-detected heteronuclear correlation using gradient-enhanced Z and Zz filters. J. Magn. Reson. **A101**, 113–117
19 Cierpicki, T. and Otlewski, J. (2001) Amide proton temperature coefficients as hydrogen bond indicators in proteins. J. Biomol. NMR **21**, 249–261
20 Cierpicki, T., Zhukov, I., Byrd, R. A. and Otlewski, J. (2002) Hydrogen bonds in human ubiquitin reflected in temperature coefficients of amide protons. J. Magn. Reson. **157**, 178–180
21 Delaglio, F., Grzesiek, S., Vuister, G. W., Zhu, G., Pfeifer, J. and Bax, A. (1995) NMRPipe: a multidimensional spectral processing system based on unix pipes. J. Biomol. NMR **6**, 277–293
22 Johnson, B. A. and Blevins, R. A. (1994) NMRView: a computer-program for the visualization and analysis of NMR data. J. Biomol. NMR **4**, 603–614
23 Wishart, D. S., Sykes, B. D. and Richards, F. M. (1992) The chemical-shift index: a fast and simple method for the assignment of protein secondary structure through NMR spectroscopy. Biochemistry **31**, 1647–1651
24 Wishart, D. S. and Sykes, B. D. (1994) The C-13 chemical-shift index: a simple method for the identification of protein secondary structure using C-13 chemical-shift data. J. Biomol. NMR **4**, 171–180
25 Hamilton, K. S., Ellison, M. J., Barber, K. R., Williams, R. S., Huzil, J. T., McKenna, S., Ptak, C., Glover, M. and Shaw, G. S. (2001) Structure of a conjugating enzyme-ubiquitin thiolester intermediate reveals a novel role for the ubiquitin tail. Structure **9**, 897–904

26 Merkley, N. and Shaw, G. S. (2004) Solution structure of the flexible class II ubiquitin-conjugating enzyme Ubc1 provides insights for polyubiquitin chain assembly. J. Biol. Chem. **279**, 47139–47147

27 Miura, T., Klaus, W., Ross, A., Guntert, P. and Senn, H. (2002) Letter to the Editor: the NMR structure of the class I human ubiquitin-conjugating enzyme 2b. J. Biomol. NMR **22**, 89–92

28 Saxena, K., Jacobs, D. M., Vogtherr, M., Grimme, S., Elshort, B., Pescatore, B., Betz, M., Schieborr, U., Langer, T., Schwalbe, H. and Fiebig, K. (2005) Backbone NMR assignment of the human E2 ubiquitin conjugating enzyme UbcH5α (F72K,F82S) double mutant. J. Biomol. NMR **32**, 338

29 Houben, K., Dominguez, C., van Schaik, F. M., Timmers, H. T., Bonvin, A. M. and Boelens, R. (2004) Solution structure of the ubiquitin-conjugating enzyme UbcH5B. J. Mol. Biol. **344**, 513–526

30 Ju, T., Bocik, W., Majumdar, A. and Tolman, J. R. (2010) Solution structure and dynamics of human ubiquitin conjugating enzyme Ube2g2. Proteins **78**, 1291–1301

31 Liu, Q., Shen, B. H., Chen, D. J. and Chen, Y. (1999) Backbone resonance assignments of human UBC9. J. Biomol. NMR **13**, 89–90

32 Mercier, P., Lewis, M. J., Hau, D. D., Saltibus, L. F., Xiao, W. and Spyracopoulos, L. (2007) Structure, interactions, and dynamics of the RING domain from human TRAF6. Protein Sci. **16**, 602–614

33 Wickliffe, K. E., Lorenz, S., Wemmer, D. E., Kuriyan, J. and Rape, M. (2011) The mechanism of linkage-specific ubiquitin chain elongation by a single-subunit E2. Cell **144**, 769–781

34 Pardi, A., Wagner, G. and Wuthrich, K. (1983) Protein conformation and proton nuclear-magnetic-resonance chemical shifts. Eur. J. Biochem. **137**, 445–454

35 Perkins, S. J. and Wuthrich, K. (1979) Ring current effects in the conformation dependent NMR chemical-shifts of aliphatic protons in the basic pancreatic trypsin-inhibitor. Biochim. Biophys. Acta **576**, 409–423

36 Eletsky, A., Heinz, T., Moreira, O., Kienhofer, A., Hilvert, D. and Pervushin, K. (2002) Direct NMR observation and DFT calculations of a hydrogen bond at the active site of a 44 kDa enzyme. J. Biomol. NMR **24**, 31–39

37 Pelton, J. G., Torchia, D. A., Meadow, N. D. and Roseman, S. (1993) Tautomeric states of the active-site histidines of phosphorylated and unphosphorylated IIIGlc, a signal-transducing protein from *Escherichia coli*, using two-dimensional heteronuclear NMR techniques. Protein Sci. **2**, 543–558

38 Bhattacharya, S., Sukits, S. F., MacLaughlin, K. L. and Lecomte, J. T. (1997) The tautomeric state of histidines in myoglobin. Biophys. J. **73**, 3230–3240

39 Bachovchin, W. W. (2001) Contributions of NMR spectroscopy to the study of hydrogen bonds in serine protease active sites. Magn. Reson. Chem. **39**, S199–S213

40 Hempelmann, F., Holper, S., Verhoefen, M. K., Woerner, A. C., Kohler, T., Fiedler, S. A., Pfleger, N., Wachtveitl, J. and Glaubitz, C. (2011) His75-Asp97 cluster in green proteorhodopsin. J. Am. Chem. Soc. **133**, 4645–4654

41 Sudmeier, J. L., Bradshaw, E. M., Haddad, K. E., Day, R. M., Thalhauser, C. J., Bullock, P. A. and Bachovchin, W. W. (2003) Identification of histidine tautomers in proteins by 2D $^{1}H/^{13}C(\delta 2)$ one-bond correlated NMR. J. Am. Chem. Soc. **125**, 8430–8431

42 Chen, V. B., Arendall, III, W. B., Headd, J. J., Keedy, D. A., Immormino, R. M., Kapral, G. J., Murray, L. W., Richardson, J. S. and Richardson, D. C. (2010) MolProbity: all-atom structure validation for macromolecular crystallography. Acta Crystallogr. Sect. D Biol. Crystallogr. **66**, 12–21

43 Gareau, J. R., Reverter, D. and Lima, C. D. (2012) Determinants of small ubiquitin-like modifier 1 (SUMO1) protein specificity, E3 ligase, and SUMO-RanGAP1 binding activities of nucleoporin RanBP2. J. Biol. Chem. **287**, 4740–4751

44 Winn, P. J., Battey, J. N., Schleinkofer, K., Banerjee, A. and Wade, R. C. (2005) Issues in high-throughput comparative modelling: a case study using the ubiquitin E2 conjugating enzymes. Proteins **58**, 367–375

45 McKenna, S., Moraes, T., Pastushok, L., Ptak, C., Xiao, W., Spyracopoulos, L. and Ellison, M. J. (2003) An NMR-based model of the ubiquitin-bound human ubiquitin conjugation complex Mms2-Ubc13. The structural basis for lysine 63 chain catalysis. J. Biol. Chem. **278**, 13151–13158

46 Sakata, E., Satoh, T., Yamamoto, S., Yamaguchi, Y., Yagi-Utsumi, M., Kurimoto, E., Tanaka, K., Wakatsuki, S. and Kato, K. (2010) Crystal structure of UbcH5b$\sim$ubiquitin intermediate: insight into the formation of the self-assembled E2$\sim$Ub conjugates. Structure **18**, 138–147

Received 23 March 2012/30 April 2012; accepted 8 May 2012
Published as BJ Immediate Publication 8 May 2012, doi:10.1042/BJ20120504

Biochem. J. (2012) **445**, 167–174 (Printed in Great Britain) doi:10.1042/BJ20120504

online data

SUPPLEMENTARY ONLINE DATA

Architecture of the catalytic HPN motif is conserved in all E2 conjugating enzymes

Benjamin W. COOK and Gary S. SHAW[1]

Department of Biochemistry, The University of Western Ontario, London, ON, Canada, N6A 5C1

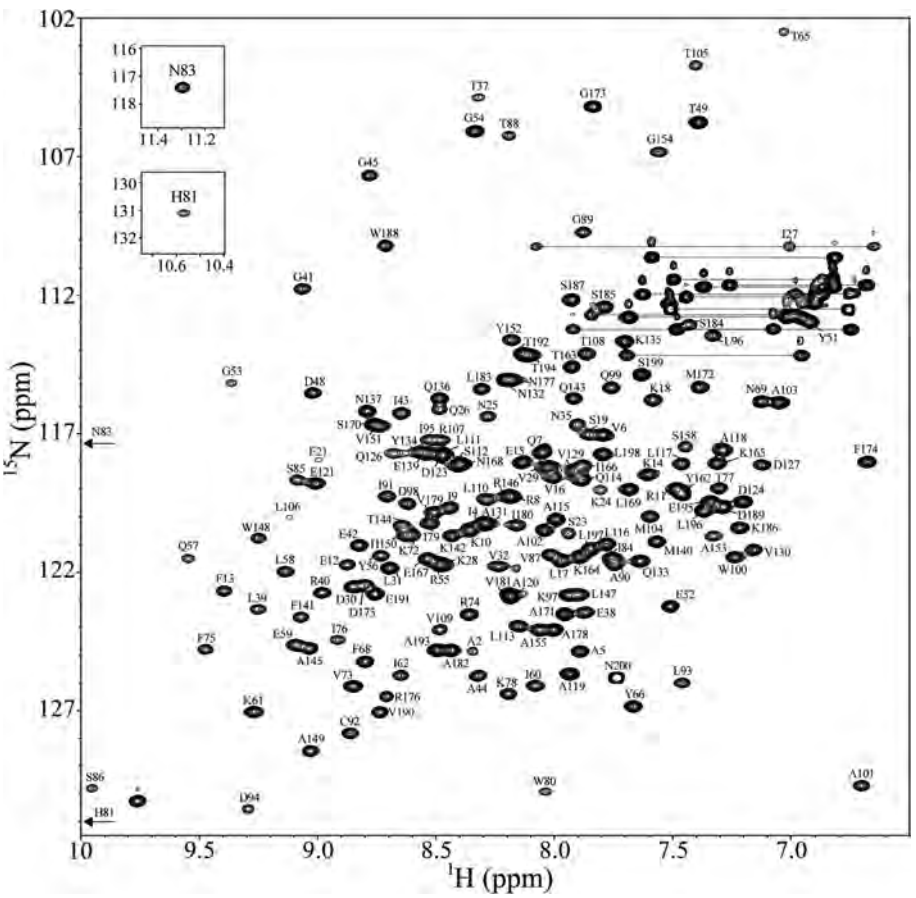

Figure S1 Assigned (^{1}H-^{15}N)-HSQC spectrum of HIP2

Backbone amide signals are labelled with amino acid single letter codes and sequence number. Signals connected by lines indicate side chain amide resonances from asparagine and glutamine residues. The signals marked with (*) represent side chain amides from tryptophan residues. The two arrows indicate signals that are shifted outside the plotted region for His^{81} and Asn^{83} (shown as insets). The spectrum was collected at 600 MHz using ^{15}N,^{13}C-labelled HIP2 (575 μM) in 10 % $^{2}H_2O$, 200 mM NaCl, 5 mM DTT, 1 mM EDTA and 25 mM Tris/HCl (pH 7.5) at 30 °C.

[1] To whom correspondence should be addressed (email gshaw1@uwo.ca).

Table S1 Crystallographic or NMR conditions of E2 conjugating enzymes

NMR conditions were acquired from the methods section of the PDB entry. PDB structures are human unless indicated. MME, mono-methyl ether; PEG, poly(ethylene) glycol.

Protein name						
IUPAC	Common	PDB code	Temperature (K)	pH	Salt	Other
UBE2K	HIP2	2BEP	295	8.5	0.1 M Tris/HCl, 0.07 M ammonium acetate	17% PEG MME 5000
	E2-25K	3E46	298	6.0	Calcium acetate, sodium acetate, NaCl	PEG 8000
		1YLA	295	6.5	Calcium acetate, cacodylate	PEG 8000
		3K9P	293	7.5	0.1 M Hepes/NaOH, 0.05 M sodium fluoride	25% PEG 3350
		2O25	298	6.0	0.1 M Bis-Tris,	16% PEG MME 5000, 0.001 M DTT
		2BF8	-	8.5	0.1 M Tris/HCl, 0.2 M $MgCl_2$	17% PEG 4000, 10% glycerol
		3K9O	293	8.5	0.1 M Tris/HCl	25% PEG 3350
UBC1	Ubc1	1TTE (yeast)	308	7.5	0.025 M Tris/HCl, 0.15 M NaCl	0.001 M EDTA, 0.001 M DTT
		1FXT (yeast)	303	7.5	0.04 M Hepes, 0.45 M NaCl, 0.005 M $MgCl_2$	0.001 M EDTA
		1FZY (yeast)	298	6.0	Ammonium sulfate, Mes buffer	Propan-2-ol, PEG 5000
UBE2B	Ubc2b	1JAS	308	6.7	0.075 M ammonium acetate, 0.1 M ammonium sulfate	-
	Rad6B	2Y4W	310	8.0	0.05 M potassium phosphate, 0.3 M NaCl	0.001 M DTT
		2YB6	-	5.5	0.2 M sodium tartrate, 0.1 M Bis-Tris, 1.6 M ammonium sulfate	-
		2YBF	-	6.5	2.2 M ammonium sulfate, 0.1 M sodium cacodylate	0.005 M 2-mercaptoethanol
		1AYZ (yeast)	-	5.0	0.05 M Mes	12% PEG 8000, 1% spermine
UBE2D1	UbcH5a	3PTF	292	8.5	0.02 M Mes, 0.15 M NaCl	0.0005 M TCEP, 24% PEG 10000
		2C4P	-	4.6	0.2 M ammonium sulfate, 0.1 M sodium acetate	25% PEG MME 2000
		3OJ4	292	7.1	0.1 M Hepes, 1.85 M sodium malonate	-
		2YHO	-	5.5	0.1 M sodium citrate, 0.2 M sodium acetate	10% PEG 4000
UBE2D2	UbcH5b	2ESK	294	4.5	NaCl, sodium acetate	PEG 6000
	E2-17K	1UR6	-	-	-	-
	Ubc4	2C4O	-	4.6	0.15 M ammonium sulfate, 0.1 M sodium acetate	25% PEG MME 2000
		1W4U	300	7.0	0.02 M potassium phosphate, 0.15 M potassium chloride	0.00001 M $ZnCl_2$
		3A33	293	4.1	2 M NaCl, 0.1 M potassium acetate	-
		3TGD	293	7.5	0.8 M potassium phosphate, 0.8 M sodium phosphate, 0.1 M Hepes	-
		2CLW	-	4.6	0.15 M ammonium sulfate, 0.1 M ammonium acetate	25% PEG MME 2000
		3L1Y	295	4.6	2 M sodium formate, 0.1 M sodium acetate	-
		3JVZ	277	5.1	0.1 M sodium citrate, 2.5 M NaCl	-
		3EB6 (frog)	291	7.3	3.3 M NaCl, 0.1 M Hepes	-
		4A4C	277	7.5	0.05 M Hepes, 0.2 M KCl	31–35% Pentaerythritol propoxylate
UBE2G2	Ubc7	2KLY	295	7.0	0.05 M NaCl	-
		2CYX	293	8.1	0.1 M Tris/HCl, 1.45 M ammonium sulfate	12% glycerol
		3FSH (mouse)	293	7.7	2.8 M sodium formate, 0.1 M Tris/HCl	0.005 M DTT
		3H8K	292	8.5	0.1 M Tris/HCl	PEG 3350
UBE2I	Ubc9	2GRN	291	5.5	1 M lithium sulfate, 0.5 M ammonium sulfate, 0.05 M sodium citrate	
		1Z5S	291	5.0	0.1 M sodium citrate, 0.2 M ammonium acetate	18% PEG 4000
		1U9B	-	6.5	0.1 M ammonium sulfate, 0.1 M Mes	23% PEG MME 5000, 9% propan-2-ol
		1A3S	-	7.0	-	-
		2O25	298	6.0	0.1 M Bis-Tris,	16% PEG MME 5000 0.001 M DTT
		2PE6	291	8.5	0.1 M Tris/HCl	25% PEG 3000
		1KPS	291	7.0	2.0 M ammonium phosphate, 0.1 M Hepes	0.01 M $CuCl_2$, 5% glycerol
		1U9A (mouse)	-	7.5	0.1 M Hepes	9% PEG 4000, 9% propan-2-ol
		2VRR	-	6.5	0.2 M sodium formate, 0.1 M Bis-Tris	24% PEG 3350
		3RCZ (yeast)	293	5.8	0.2 M imidazole-malate, 0.6 M lithium nitrate	20% PEG 8000, 0.001 M DTT
		2GJD (yeast)	291	7.5	0.1 M Hepes, 0.1 M sodium bromide	18% PEG 6000, 0.005 M DTT
		2XWU	-	6.5	0.05 M Mes	25% PEG 300
		2UYZ (mouse)	-	5.5	0.1 M Bis-Tris	16.5% PEG 3350, 15% glycerol
		3ONG (yeast)	277	5.5	0.1 M Bis-Tris, 0.2 M lithium sulfate	20% PEG 3350
		3A4S	277	6.0	0.1 M SPG buffer	25% PEG 1500
		3UIN	279	7.5	0.1M Hepes, 0.4 M ammonium citrate	2% propan-2-ol
UBE2L3	UbcH7	1C4Z	277	6.5	$MgCl_2$, Mes	PEG 1500
		1FBV	277	5.6	0.1 M sodium citrate, 2 M ammonium sulfate	-
		3SQV	298	6.0	1.6 M ammonium sulfate, 0.1 M Mes	-
		3SY2	298	6.5	0.1 M Mes, 1.6 M ammonium sulfate	-
UBE2L6	UbcH8	1WZW	298	7.3	Calcium acetate	PEG 3350
		1WZV	298	7.3	Calcium acetate	PEG 3350
		1WZV	298	7.3	Calcium acetate	PEG 3350
		2KJH	298	7.4	0.02 M sodium phosphate, 0.25 M NaCl	0.001 M EDTA, 0.05 M arginie/glutamate
UBE2N	Ubc13	1J7D	298	6.5	0.1 M sodium citrate	20% PEG 8000
		2C2V	293	7.0	0.1 M Tris/HCl	20% PEG MME 2000
		3HCT	298	7.5	-	8% PEG 4000
		3HCU	293	8.5	0.2 M $MgCl_2$	18% PEG 4000
		2GMI (yeast)	277	6.2	0.1 M sodium/potassium phosphate, 0.025 M NaCl	17% PEG 1000
		1JBB (yeast)	298	6.0	0.2 M ammonium sulfate	30% PEG MME 5000
		1JAT (yeast)	298	7.5	Tris/HCl	PEG 1000

Table S1 Continued

Protein name						
IUPAC	Common	PDB code	Temperature (K)	pH	Salt	Other
UBE2R1	Cdc34	2OB4	294	8.5	7.5 M gly-gly-glycine, 0.2 M $MgCl_2$, 0.1 M Tris/HCl, 0.2 M $MgCl_2$	28 % PEG 4000, 0.001 M DTT
		3RZ3	293	8.0	0.5 M sodium phosphate, 1.6 M potassium phosphate, 0.2 M NaCl	0.1 M imidazole
UBE2S	E2-EPF	1ZDN	298	6.5	3 M sodium formate, 0.1 M Bis-Tris	-
UBE2T	HSPC150	1YH2	298	-	4 M sodium formate	-
UBE2U		1YRV	298	7.0	0.1 M Hepes	10 % PEG MME 5000, 5 % tacsimate 5
UBE2C	UbcH10	1I7K	293	7.0	NaCl, sodium acetate	30 % PEG 1500
UBE2D3	UbcH5c	3RPG	277	6.0	0.1 M Mes	40 % Methylpropanediol
		3L1Z	295	-	4 M sodium formate	-
		2FUH	298	7.0	0.15 M NaCl	-
UBE2G1	Ube2g	2AWF	298	7.5	0.2 M magnesium acetate, 0.1 M Tris/HCl	24 % PEG 3350, 5 % glycerol
UBE2H	UbcH	2Z5D	290	5.5	0.2 M NaCl, 0.1 M Bis-Tris	25 % PEG 3350
		2ONU (protozoan)	291	8.5	0.1 M Ammonium sulfate, 0.1 M Tris/HCl	25 % PEG 3350
UBE2F	NCE2	2EDI	293	7.0	0.02 M Tris/HCl, 0.1 M NaCl	0.001 M DTT
		3FN1	291	9.0	0.75 M sodium citrate, 0.2 M NaCl	0.1 M Bicine, 0.005 M DTT
UBE2M	Ubc12	1Y8X	277	5.5	0.1 M ammonium sulfate, 0.1 M Bis-Tris	14 % PEG 3500, 0.005 M DTT
		2NVU	291	7.0	0.1 M Hepes, 0.2M disodium tartrate	17 % PEG 3350

Table S2 Structural analysis of the HPN histidine-asparagine bond within E2 conjugating enzymes

PDB structures are human unless indicated. PDB structure 1WZV is listed twice representing model A (correct) and model B (reorientation suggested).

Protein Name							
IUPAC	Common	PDB	Method	Resolution (Å)	$N^{\delta1}$-N distance (Å) (Figure 2A of the main text)*	$N^{\varepsilon2}$-$O^{\delta1}$ distance (Å) (Figure 2B of the main text)*	MolProbity analysis [1] (HPN histidine orientation)
UBE2K	HIP2	2BEP	X-ray	1.80	2.99		Correct
	E2-25K	3E46	X-ray	1.86		3.25	Reorientation suggested
		1YLA	X-ray	2.40		3.18	Reorientation suggested
		3K9P	X-ray	2.80		3.00	Reorientation suggested
		2O25	X-ray	2.60		3.75	Reorientation suggested
		2BF8	X-ray	2.30	3.06		Correct
		3K9O	X-ray	1.80		3.20	Reorientation suggested
UBC1	Ubc1	1TTE (yeast)	NMR		Variable	Variable	N/A: both orientations
		1FXT (yeast)	NMR			2.99	Correct‡
		1FZY (yeast)	X-ray	1.90		3.16	Reorientation suggested
UBE2B	Ubc2b	1JAS	NMR		Variable		Correct
	Rad6B	2Y4W	NMR		Variable	Variable	N/A: both orientations
		2YB6	X-ray	1.50	2.93		Correct
		2YBF	X-ray	2.00	3.07		Correct
		1AYZ (yeast)	X-ray	2.60		3.03	Reorientation suggested
UBE2D1	UbcH5a	3PTF	X-ray	2.70	2.96		Correct
		2C4P	X-ray	2.35		3.07†	Correct‡
		3OJ4	X-ray	3.40	2.99		Correct
		2YHO	X-ray	2.10	3.04		Correct
UBE2D2	UbcH5b	2ESK	X-ray	1.36	2.92		Correct
	E2-17K	1UR6	NMR		Variable		Correct
	Ubc4	2C4O	X-ray	1.94		3.22†	Reorientation suggested
		1W4U	NMR		Variable	Variable	N/A: both orientations
		3A33	X-ray	2.20	2.99		Correct
		3TGD	X-ray	1.80	2.99		Correct
		2CLW	X-ray	1.95	2.86		Correct
		3L1Y	X-ray	1.60	2.98		Correct
		3JVZ	X-ray	3.30	2.74		Correct
		3EB6 (frog)	X-ray	3.40	2.98		Correct
		4A4C	X-ray	2.70		3.38	Reorientation suggested
UBE2G2	Ubc7	2KLY	NMR		Variable		Correct
		2CYX	X-ray	2.56	2.95		Correct
		3FSH (mouse)	X-ray	2.76	2.97		Correct
		3H8K	X-ray	1.80	2.94		Correct

Table S2 Continued

Protein Name							
IUPAC	Common	PDB	Method	Resolution (Å)	$N^{\delta 1}$-N distance (Å) (Figure 2A of the main text)*	$N^{\varepsilon 2}$-$O^{\delta 1}$ distance (Å) (Figure 2B of the main text)*	MolProbity analysis [1] (HPN histidine orientation)
UBE2I	Ubc9	2GRN	X-ray	1.80	2.90		Correct
		1Z5S	X-ray	3.01	2.70		Correct
		1U9B	X-ray	2.00	2.86		Correct
		1A3S	X-ray	2.80	2.95		Correct
		2O25	X-ray	2.60	3.02		Correct
		2PE6	X-ray	2.40	2.90		Correct
		1KPS	X-ray	2.50	2.77		Correct
		1U9A (mouse)	X-ray	2.00	2.90		Correct
		2VRR	X-ray	2.22	2.97		Correct
		3RCZ (yeast)	X-ray	1.90		3.37	Reorientation suggested
		2GJD (yeast)	X-ray	1.75	2.96		Correct
		2XWU	X-ray	2.80	2.88		Correct
		2UYZ (mouse)	X-ray	1.40	2.93		Correct
		3ONG (yeast)	X-ray	2.30	3.03		Correct
		3A4S	X-ray	2.70	3.02		Correct
		3UIN	X-ray	2.60	3.08		Correct
UBE2L3	UbcH7	1C4Z	X-ray	2.60		3.31†	Reorientation suggested
		1FBV	X-ray	2.90		5.94	Reorientation suggested
		3SQV	X-ray	3.30		4.58†	Reorientation suggested
		3SY2	X-ray	3.27		3.12†	Reorientation suggested
UBE2L6	UbcH8	1WZW	X-ray	2.40	3.12		Correct
		1WZV	X-ray	2.10	3.11		Correct
		1WZV	X-ray	2.10		3.41†	Reorientation suggested
		2KJH	NMR		Variable		Reorientation suggested‡
UBE2N	Ubc13	1J7D	X-ray	1.85	2.92		Correct
		2C2V	X-ray	2.90		3.38	Reorientation suggested
		3HCT	X-ray	2.10	2.89		Correct
		3HCU	X-ray	2.60	2.58		Correct
		2GMI (yeast)	X-ray	2.50		3.21	Reorientation suggested
		1JBB (yeast)	X-ray	2.00		3.35†	Reorientation suggested
		1JAT (yeast)	X-ray	1.60		3.25†	Reorientation suggested
UBE2R1	Cdc34	2OB4	X-ray	2.40	3.06		Correct
		3RZ3	X-ray	2.30	2.86		Correct
UBE2S	E2-EPF	1ZDN	X-ray	1.93	2.91		Correct
UBE2T	HSPC150	1YH2	X-ray	2.00	2.89		Correct
UBE2U		1YRV	X-ray	2.18	2.90		Correct
UBE2C	UbcH10	1I7K	X-ray	1.95	2.89		Correct
UBE2D3	UbcH5c	3RPG	X-ray	2.65	2.84		Correct
		3L1Z	X-ray	3.17	2.86		Correct
		2FUH	NMR		Variable	Variable	N/A: both orientations
UBE2G1	Ube2g	2AWF	X-ray	2.10	2.91		Correct
UBE2H	UbcH	2Z5D	X-ray	2.10	2.94		Correct
		2ONU (protozoan)	X-ray	2.38	3.09		Correct
UBE2F	NCE2 (nedd8 E2)	2EDI	NMR		Variable		Correct
		3FN1	X-ray	2.50		3.46	Reorientation suggested
UBE2M	Ubc12	1Y8X	X-ray	2.40		3.17	Reorientation suggested
		2NVU	X-ray	2.80	2.98		Correct

*Histidine $N^{\delta 1}$ or $N^{\varepsilon 2}$ hydrogen-bonding distance to asparagine N, $O^{\delta 1}$ or $N^{\delta 2}$ represents the N–N, N–O and N–N distance.
†These distances represent histidine $N^{\varepsilon 2}$/asparagine $N^{\delta 2}$ N–N distances whereby the asparagine side chain is incorrectly orientated.
‡Rare cases where the asparagine side chain/histidine $N^{\varepsilon 2}$ hydrogen bond is preferred by MolProbity.

REFERENCE

1 Chen, V. C., Arendall, III, W. B., Headd, J. J., Keedy, D. A., Immormino, R. M., Kapral, G. J., Murray, L. W., Richardson, J. S. and Richardson, D. C. (2010) MolProbity: all-atom structure validation for macromolecular crystallography. Acta Crystallogr. Sect. D Biol. Crystallogr. **66**, 12–21

Received 23 March 2012/30 April 2012; accepted 8 May 2012
Published as BJ Immediate Publication 8 May 2012, doi:10.1042/BJ20120504